Ocean Model Diagnostics

Robert Marsh

National Oceanography Centre, Southampton
University of Southampton

Abstract

Sea Surface Temperature (SST) exerts a key influence on the atmosphere. The focus here is on SST anomalies in the extra-tropics. On timescales from months to decades, the ocean may play an important role in shaping SST anomaly patterns through both storage and transport of heat content anomalies that are later expressed at the surface. Ocean models and fully-coupled climate models of increasing fidelity are used to investigate the associated oceanic and coupled processes. SST variability on seasonal and decadal timescales may be associated with quite distinct processes - SST 'reemergence' and internal variability of the meridional overturning circulation respectively - although both processes may operate at interannual timescales, alongside coupled modes of gyre variability. Standard and innovative ocean model diagnostics are used in combination to investigate individual processes and their integral effects. There is a clear distinction between Eulerian and Lagrangian diagnostics, the latter encompassing tracers and particle trajectrories, as well as more innovative approaches to the phenomenon of 'remote reemergence' of SST anomalies.

1.   Introduction

The ocean may be regarded as a 'passive' or 'active' participant in climate variability. The corresponding variability of sea surface temperature (SST), as evident in satellite passive microwave measurements (Deser et al., submitted) may therefore be regarded as arising through an oceanic cause or an atmospheric effect. Such SST variability can be characterized by different timescale-dependent spatial modes. For example, the active ocean largely causes the Atlantic Multi-decadal Oscillation, while the passive ocean is largely affected by interannual variability associated with the North Atlantic Oscillation.

The focus of this contribution is on the active role of the ocean in the variability of SST in the extratropics, although the effect of the ocean on sea ice is important for climate variability at high latitudes, and coupled modes such as ENSO dominate climate variability at low latitudes. The active role of the ocean is associated with a 'memory' that exceeds a typical e-folding timescale (~3 months) for the decay of SST anomalies, based on the stochastic model of Frankignoul and Hasselmann (1977). The useful predictability that arises from this oceanic memory underpins several seasonal and decadal forecast systems presently in development.

A wide range of Ocean General Circulation Models (OGCMs) and diagnostics are presently used in such forecast systems. Distinctly different physical ocean processes govern SST variability on seasonal and decadal timescales, although SST variability at interannual timescales likely involves a mixture of these processes. Selected examples of SST variability, associated ocean processes, and relevant diagnostics are discussed in this lecture. The focus is very much a personal view, drawn to a large extent from research of the author and close colleagues.

2.   OGCMs and Diagnostics - A Brief Overview

OGCMs are principally distinguished by the vertical coordinate. Traditionally, there are three different ways to represent vertical structure: levels; layers; terrain following. The majority of OGCMs in current use are level models, although some promising results have been achieved with a new hybrid vertical coordinate the combines the advantages of levels in the upper ocean and layers in the deep ocean (Bleck, 2002). The heritage of level models has been dubbed the 'GFDL Genealogy', with origins in the late 1960s and culminating in achievements such as a global eddy-resolving simulation with OCCAM, the Ocean Circulation and Climate Advanced Model (see Fig. 1).
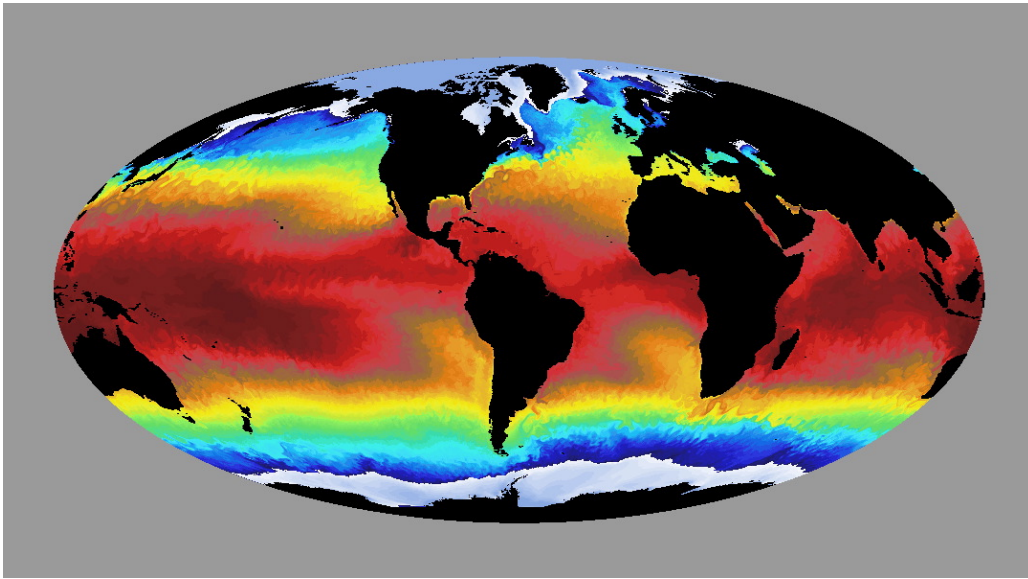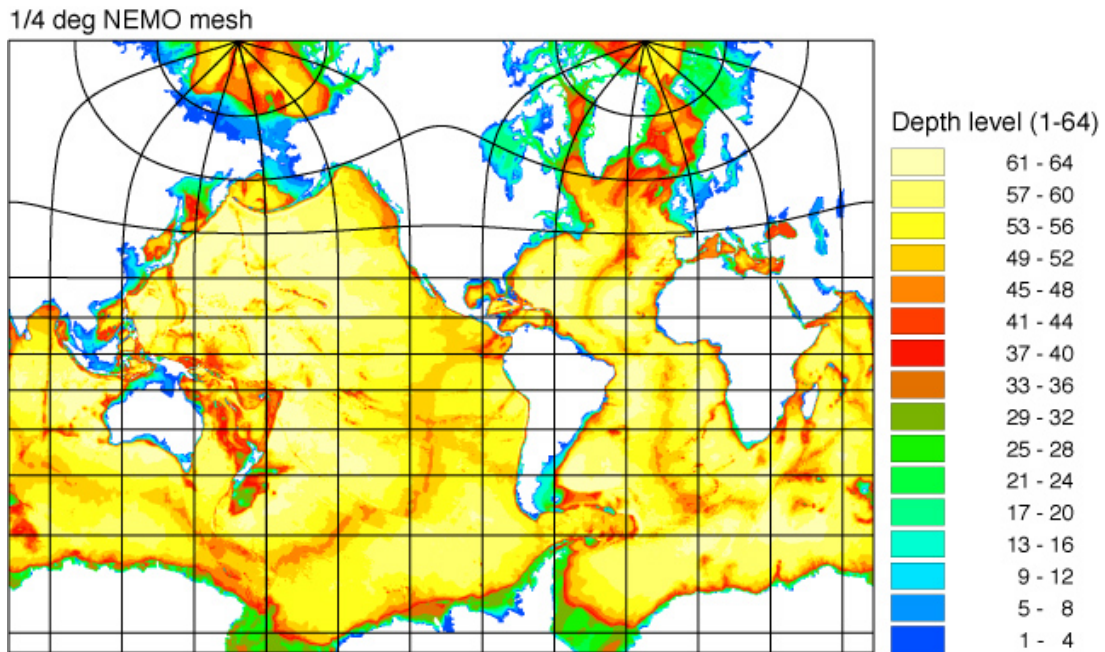

Figure 1. Sea Surface Temperature field from the 1/12° OCCAM – state of the art resolution in global ocean modelling. (Figure courtesy of Andrew Coward, National Oceanography Centre)

A recent European development is The Nucleus for European Modelling of the Oceans (NEMO), a consortium between CNRS, Mercator-Ocean, UKMO & NERC (see http://www.nemo-ocean.eu/). It is now standard practise to undertake global hindcasts with NEMO at eddy-permitting resolution (see Fig. 2). However, given inherent limitations and persistent model errors (see Section 6), the OGCM may yet be 're-invented' through innovations such as unstructured, dynamic, finite-element meshes (Pain et al., 2005; Piggott et al., 2008).

Some standard diagnostics of OGCMs share much in common with those developed for atmospheric GCMs. As in the atmosphere, transports in the vertical-meridional plane play a key role in the ocean. The Meridional Overturning Circulation (MOC) – see Fig. 3 – thought to vary at predominantly decadal timescales, can be defined as the maximum or minimum of a streamfunction for a basin bound by eastern and western boundaries:

1/4 deg NEMO mesh

Depth level (1-64)

	61 - 64
	57 - 60
	53 - 56
	49 - 52
	45 - 48
	41 - 44
	37 - 40
	33 - 36
	29 - 32
	25 - 28
	21 - 24
	17 - 20
	13 - 16
	9 - 12
	5 - 8
	1 - 4

[lines of latitude per 15 deg, lines of longitude per 30 deg]

Figure 2. Depth levels (1-64) for the 1/4° global configuration of NEMO, also illustrating the tripoolar grid.
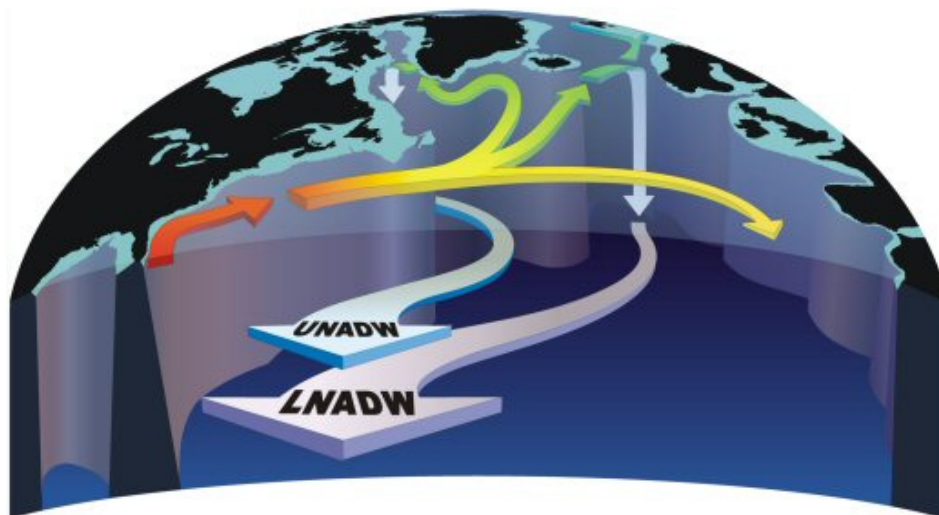

Figure 3. Three-dimensional structure of the large-scale Atlantic circulation, indicating the meridional overturning (Upper and Lower North Atlantic Deep Water) and horizontal gyre components. (Figure at http://www.noc.soton.ac.uk/rapid/sis/atlantic_conveyor.php)

$$\psi(y,z) = \int_{surface}^{z} \int_{east}^{west} v(y)dxdz \tag{1}$$

In addition to the MOC, the ocean circulates in the horizontal plane (see Fig. 3). At a given latitude, y, the meridional heat transport, Q, can therefore be decomposed as:

$$Q(y) = \rho C_p \int_z L_x [v][T]dz + \rho C_p \int_z L_x [v'T']dz \tag{2}$$

where zonal-mean temperature,

$$[T](y,z) \equiv \frac{1}{L_x(y,z)} \int_{x_w}^{x_E} T(x,y,z) \, dx$$

given basin width,

$$L_x(y,z) \equiv x_E(y,z) - x_W(y,z)$$

and local temperature anomaly,

$$T'(x,y,z) \equiv T(x,y,z) - [T](y,z)$$

The first term in (2) is attributed to the MOC, while the second 'non-MOC' term is attributed to the horizontal circulation. Although this term can be further decomposed into component attributed to large-scale gyre and mesoscale eddies, at most latitudes the gyre component is dominant. The relative importance of the MOC and non-MOC component of meridional heat transport in OGCM simulations is dependent on model resolution, with more realistic partitioning diagnosed at higher resolution (see Fig. 4).

In combination, the large-scale circulation and the seasonal cycle of mixed layer deepening/shoaling lead to exchanges of fluid between the seasonally-mixed upper layer and the main thermocline that is isolated from seasonal effects. Integrating over the annual cycle, a kinematic annual subduction rate, S_{ann} (m year^{-1}), is diagnosed as:

$$S_{ann} = \frac{1}{\tau_{year}} \int_{W1}^{W2} (\mathbf{u}_h . \nabla h + w_h)dt \tag{3}$$

where $W1$ and $W2$ denote successive winters, h is winter mixed layer depth, $\mathbf{u}_h$ is horizontal velocity at depth h, and w_h is vertical velocity at depth h.

An example of the annual subduction rate in the North Atlantic is shown in Fig. 5, revealing a band of subduction oriented from southwest to northeast across the subtropical gyre, with a region of 'obduction' (from the thermocline to the mixed layer) located to the north. Strong subduction or obduction can overwhelm the seasonal re-emergence of SST anomalies (see Section 5). The consequence of subduction is thermocline ventilation, revealed in OGCMs through property patterns (e.g., Fig. 6) or suitable tracers (e.g., Williams et al., 1995).
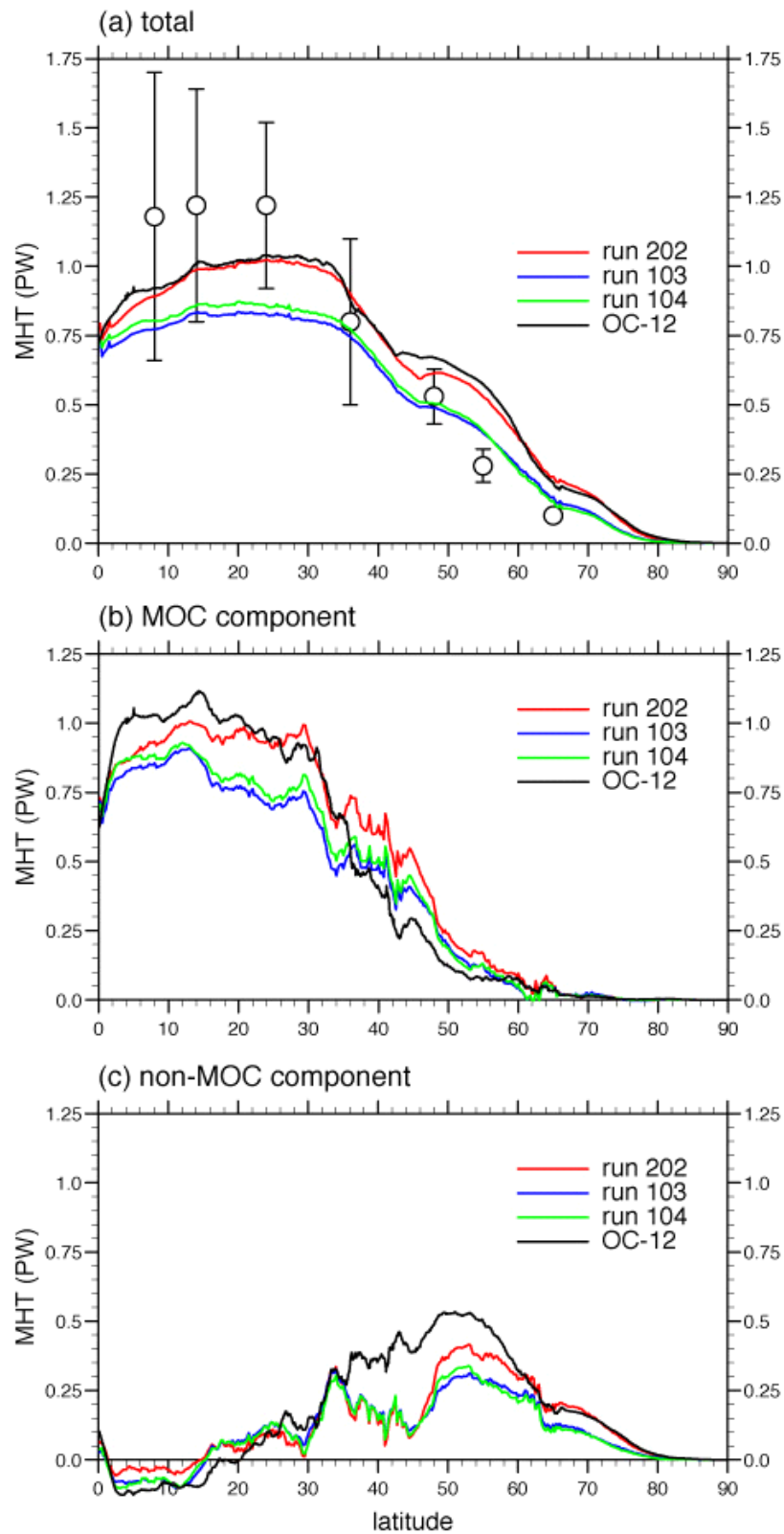
Figure 4. Decomposing Atlantic meridional heat transport (PW) in four versions of OCCAM: Runs 202, 103 and 104 are obtained with the 1/4° version of OCCAM; OC-12 is the 1/12° version (Marsh et al. 2009).
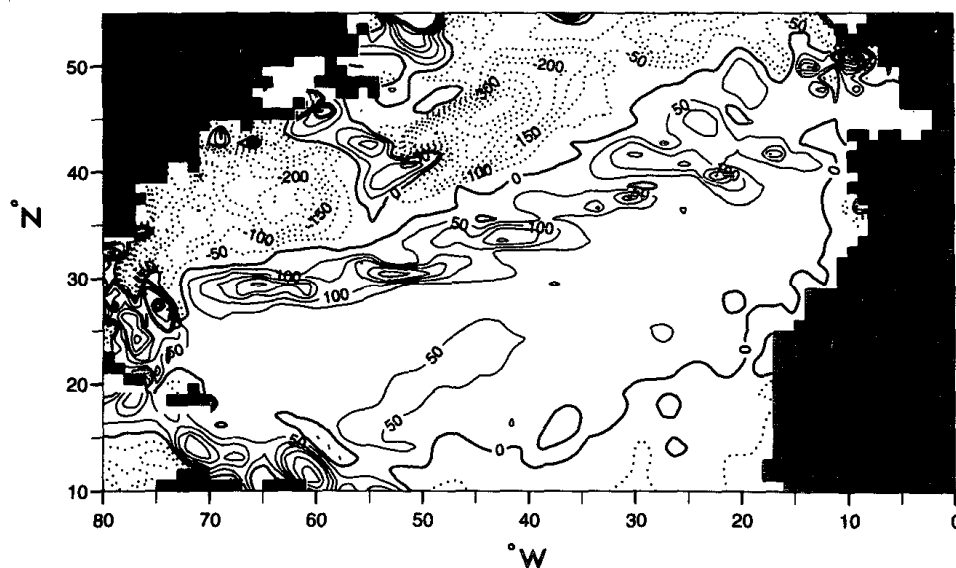
Figure 5. Annual subduction rate (m year^{-1}) across the subtropical gyre in an isopycnic model of the Atlantic (New et al. 1995).

In addition to Eulerian diagnostics, a wide range of Lagrangian diagnostics are used to highlight circulation pathways, timescales and processes. One recent innovation is an analytical method for the off-line generation of large ensembles of particle trajectories (see Marsh and Megann 2002, and references therein), used to investigate otherwise elusive processes. An example of such a process is the slow mixing and upwelling of deep water throughout the World Ocean that closes the 'Conveyor Belt' circulation (Fig. 7), although the method may provide a Lagrangian perspective on a wide range of other processes, on timescales as short as seasonal.

SAMW and AAIW layers in Southern Ocean of GIM:

(a) Layer 6 (potential density 26.52)

(b) Layer 7 (potential density 26.80)

(c) Layer 8 (potential density 27.03)

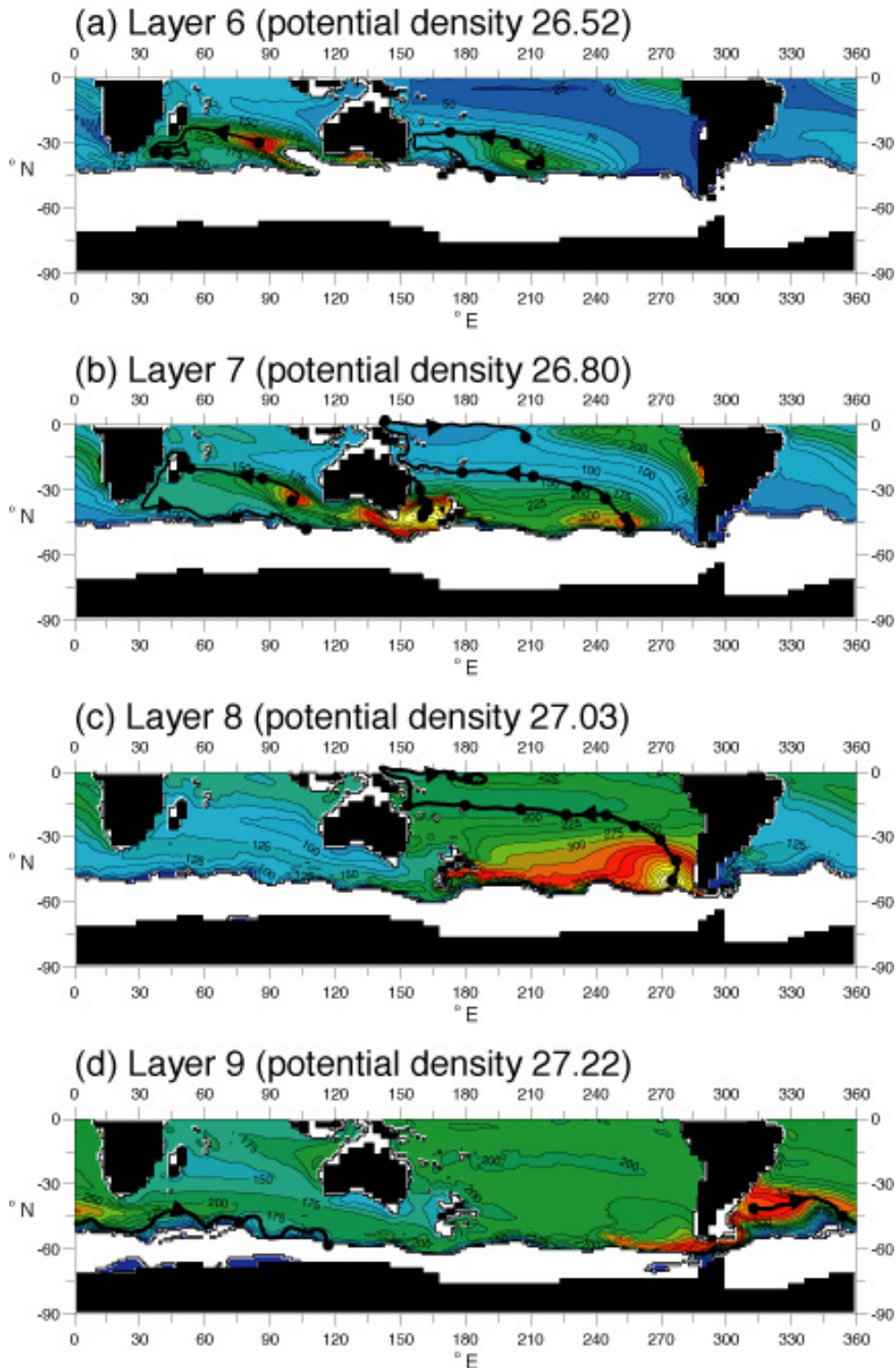### (d) Layer 9 (potential density 27.22)

Figure 6. Subduction of thick pycnostads (contouring layer thickness, m) representing Subantarctic Mode Water (SAMW) in the Southern Ocean (Marsh et al. 2000). SAMW of different densities forms where the corresponding isopycnic layer outcrops into the mixed layer with maximum thickness Selected trajectories indicate the recirculation of SAMW on a timescale indicated by the dots (plotted at 5 year intervals).
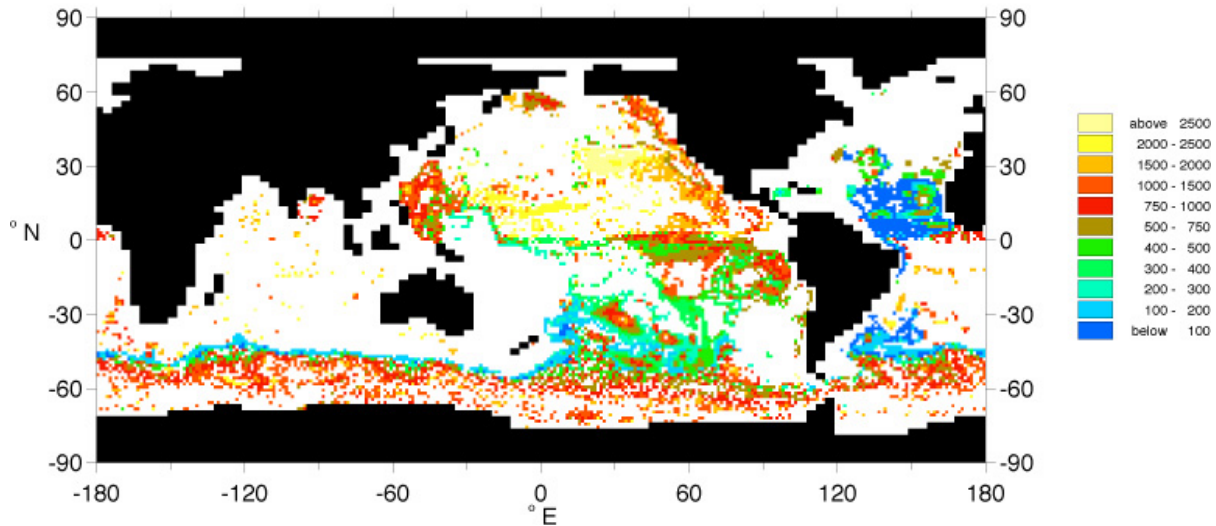
Figure 7. Closing the global circulation: age (years) of upwelling deep waters in the World Ocean determined with offline particle trajectories (Marsh and Megann 2002).

3.   Progress in Ocean Observation

Ocean model experiments and diagnostics are, of course, motivated by observations. Where the ocean is an active participant in climate variability, SST and sub-surface temperature anomalies are strongly linked. Until recently however, the sub-surface ocean was rather poorly sampled. The international Argo profiling float programme (http://www.argo.ucsd.edu/) has dramatically improved the situation, with the first floats deployed in 1999 and full target observation density achieved by 2007, with just over 3000 floats presently distributed throughout the World Ocean.

A wide range of studies has now been undertaken using Argo data. Time series of ocean heat content (OHC) have been developed for selected layers and zones or regions (e.g., Ivchenko et al., 2006). OHC anomalies estimated from Argo data can be interpreted as thermosteric height changes. Comparison with contemporaneous satellite altimetric data suggest that OHC change is the dominant factor in sea level variability at sub-decadal timescales (Fig. 8).
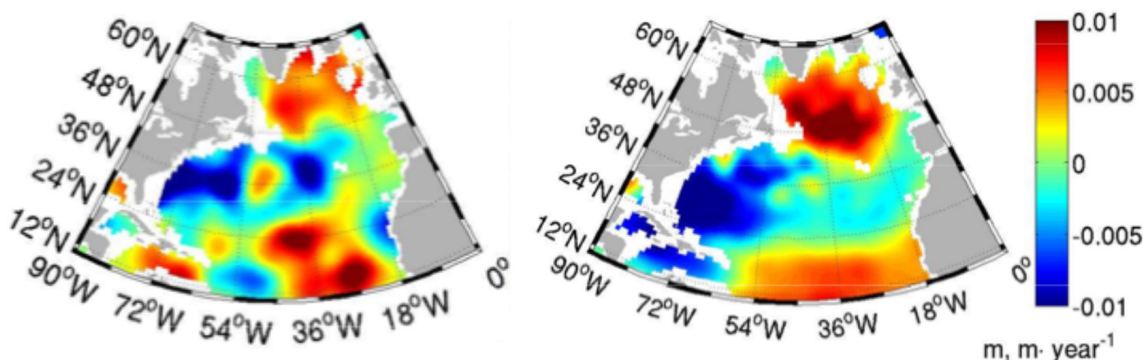

Figure 8. Trends (m year-1) over 1999-2006: (left) steric height trend, computed from Argo data; (right) SSH trend, computed from altimetric data (Ivchenko et al., 2008).
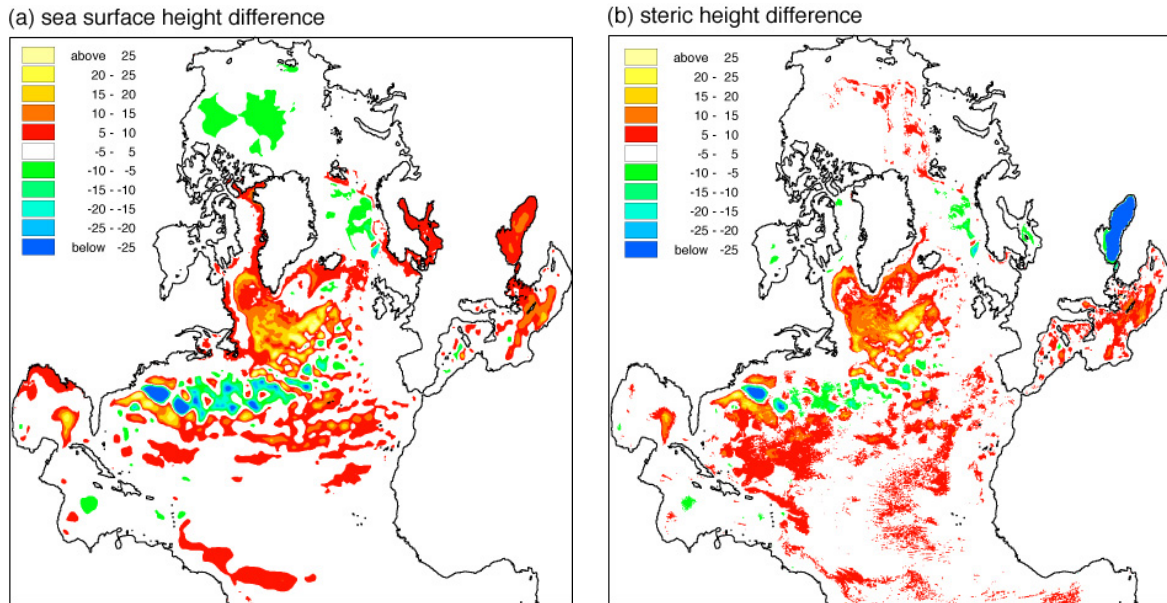
Figure 9. Changes (cm) of Sea Surface Height (left panel) and Steric height, based on changes in temperature and salinity (right panel), from 1993 (start of altimeter era) to 2004, in the 1/12° version of OCCAM.

This co-use of Argo and altimetry data motivates a similar analysis of models (Fig. 9). In such models, we may further partition OHC change between changes in surface fluxes and heat transport divergence (Marsh et al. 2008, Grist et al., 2010). Through a synthesis of in-situ data and ocean models, satellite data may provide real-time information on interannual-to-decadal changes in ocean circulation and air-sea interaction. The mechanism for such changes over recent decades is most convincingly revealed through assimilation of 3-D observations in ocean re-analysis (e.g., Balmaseda et al. 2007) or state estimation based on an adjoint approach (e.g., the ECCO project, see http://ecco.jpl.nasa.gov/external/index.php). The most profound effect on OHC in the North Atlantic is associated with decadal variability of the MOC.

4.   The Varying Meridional Overturning Circulation

The MOC plays a key role in the climate system through the associated heat transport, northward throughout the Atlantic sector (see Fig. 10, from Bryden and Imawaki, 2001). Until recently, our knowledge of the Atlantic MOC was restricted to estimates at a few selected latitudes, based on occasional hydrographic sections. The latitude most frequently occupied is 26°N, with hydrographic sections undertaken in 1957, 1981, 1992, 1998 and 2004. On the basis of MOC estimates for these five sections, Bryden et al. (2005) suggested that the MOC slowed over recent decades, most markedly since the early 1990s (Fig. 11, points with error bars). Since April 2004, an innovative monitoring array has been established at 26°N, providing essentially continuous MOC estimates (Fig. 11, red trace). The extent to which the relatively short time series is representative of MOC variability can be appreciated by considering the corresponding MOC diagnostic from a state-of-the-art ocean model, OCCAM (Fig. 11, black trace). It appears that the seasonal cycle evident in the three years for which we have continuous observations (2004-07) is not necessarily representative of a longer period (1988-2006), during which there are periods when the MOC is more characterized by a trend (e.g., 1994-97).
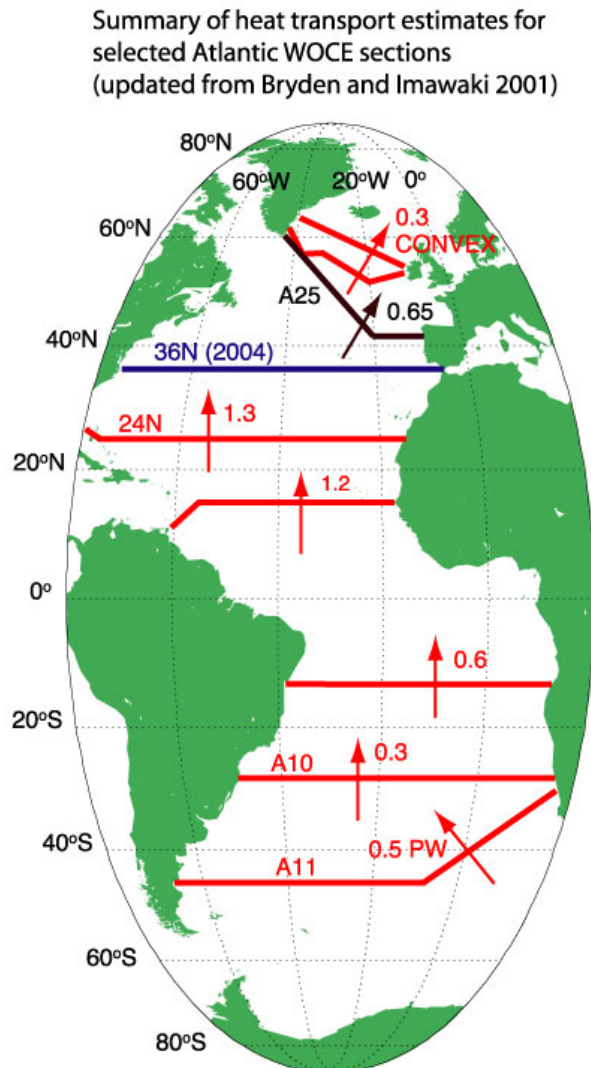
Summary of heat transport estimates for
selected Atlantic WOCE sections
(updated from Bryden and Imawaki 2001)

Figure 10. Heat transport (PW) through the Atlantic sector, as observed at selected hydrographic sections, from Bryden and Imawaki (2001).

Having established real-world MOC variability for the first time, a link has been found between MOC anomalies at 26°N and SST variability remote from the section in the tropics and at mid-latitudes, with significant correlations on time-lags of up to 6 months (Joel Hirschi, pers. comm.). Further diagnosis of the OCCAM simulation may help to explain the oceanic mechanism by which seasonal SST variability may be linked to the MOC. In complementary work, we are addressing MOC variability at other latitudes, and on longer timescales.
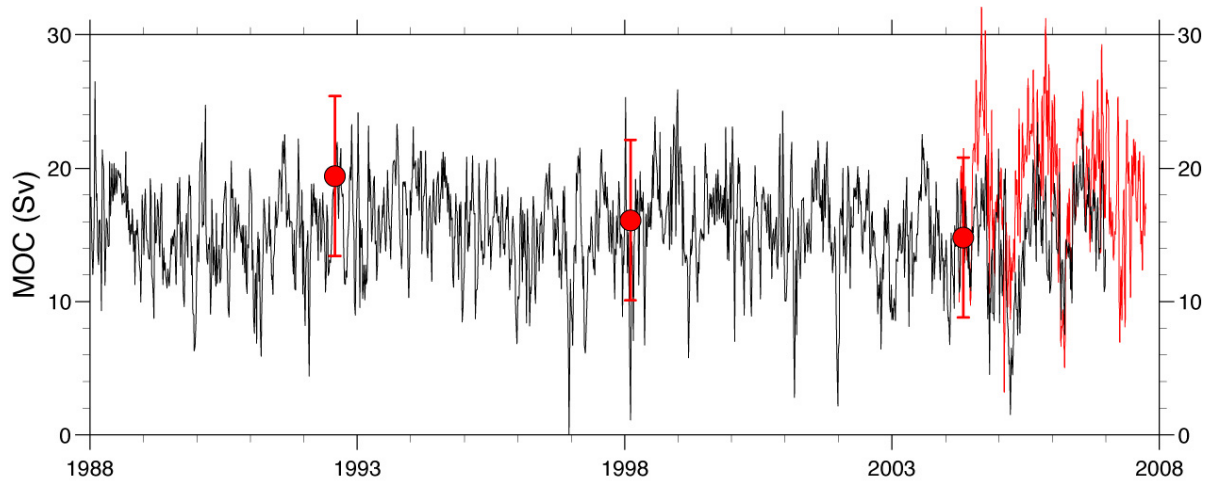
Figure 11. Overturning (Sv) at 26°N in the Atlantic: Occasional hydrographic sections, as of 2004 (red point with error bars, from Bryden et al. 2005); RAPID monitoring since April 2004 (red trace, twice daily) and 1/12° OCCAM (black trace, 5-day averages), 1988-2006.
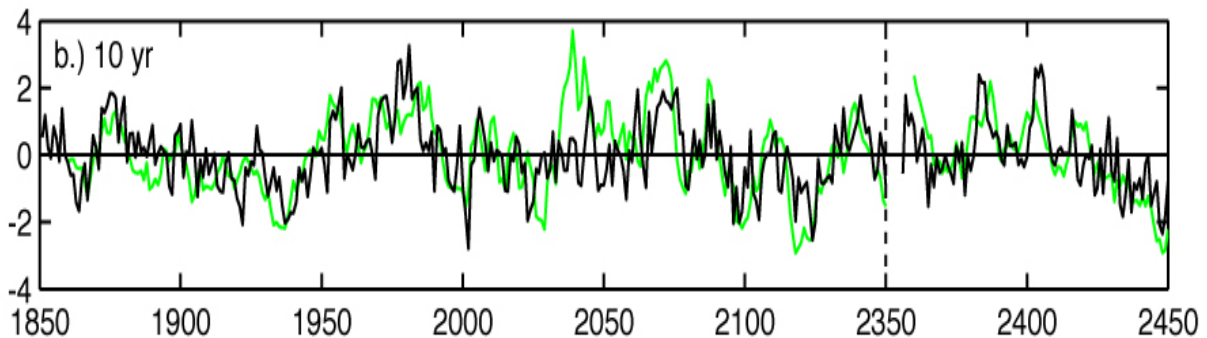

Figure 12. Overturning anomaly (Sv) at 48°N for 300-year period of HadCM3 control simulation: full MOC (black curve); SFOC (green curve) (Grist et al. 2009).

A method for diagnosing the 'surface-forced overturning circulation' (SFOC) based on water mass transformation theory (Marsh, 2000) has been further tested using three climate models – HadCM3, GFDL, Bergen Climate Model – the first two with z-coordinate oceans, the latter with an isopycnic ocean. This method for reconstructing the MOC is most successful in mid-latitudes. SFOC estimates of the MOC at 48°N are in best agreement with the full MOC in HadCM3 (Fig. 12, from Grist et al. 2009). An extension of the reconstruction method involves 'past-averaging' of surface buoyancy fluxes, and the best SFOC-MOC agreement at latitudes north (south) of 48°N is obtained with a shorter (longer) past-averaging interval (Josey et al. 2009). Having established the fidelity of this new method with climate models, MOC variability over the last 40 years can be estimated with a degree of confidence (Fig. 13, from Josey et al. 2009).
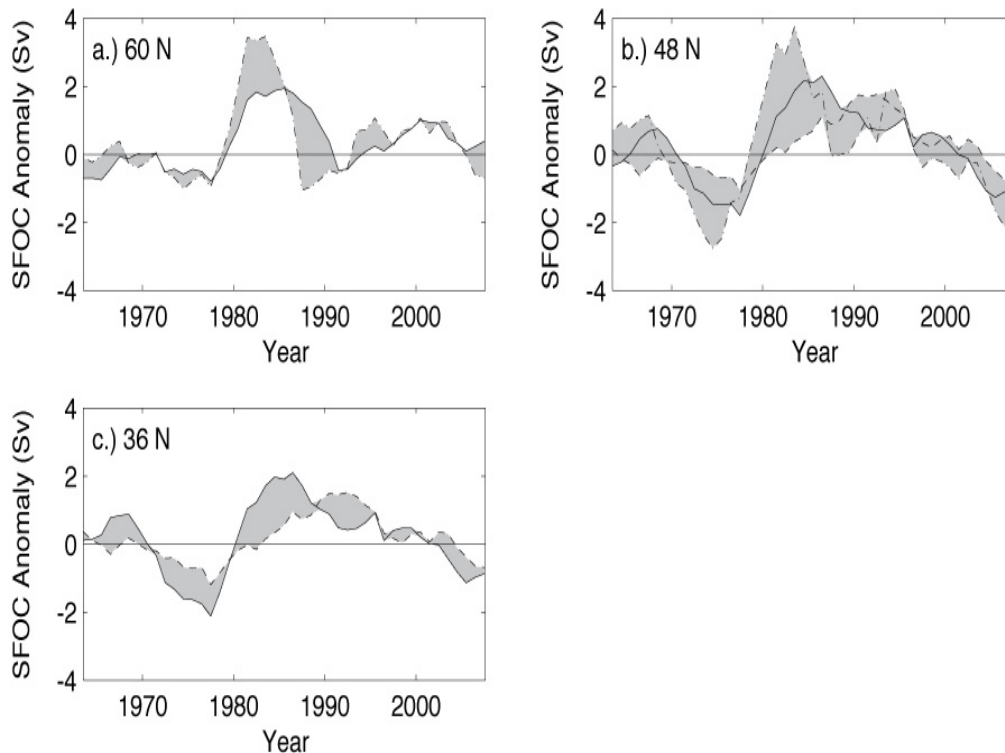
Figure 13. Reconstructed SFOC anomaly (Sv) at selected latitudes for 1965-2008 determined from the NCEP/CAR reanalysis (Josey et al. 2009). In each case, time series for different combinations of past averaging interval are shown and the grey shaded area indicates the range of uncertainty in the reconstructed value arising from reasonable choices for the past averaging interval: (a) 60ºN, 6-year averaging interval (dash-dot black line) and 10-year (solid black line) ; (b) 48ºN, 6-year (dash-dot black), 10-year (solid black) and 15-year (dashed black) ; (c) 36ºN 10-year (solid black) and 15-year (dashed black).

5. SST Reemergence in Observations and Models

While the MOC may exert an influence on SST at a seasonal timescale, details of the associated processes remain unclear. In contrast, the seasonal mixed layer cycle exerts a clearer influence on SST anomalies at seasonal to interannual timescales (Fig. 14). Some key literature concerning this process is briefly reviewed here.

Following an earlier observation of the tendency for SST anomalies to recur from one winter to the next (Namias and Born, 1970, 1974), Alexander and Deser (1995) used Ocean Weather Ship temperature observations from the North Pacific and the North Atlantic to confirm the link between SST and sub-surface temperature anomalies, and dubbed the process 'reemergence'. In subsequent studies, the same authors and colleagues established how sub-surface temperature variability extends SST predictability (Alexander et al., 1999; Alexander et al., 2001; Timlin et al., 2002; Deser et al., 2003) and the impact on atmospheric modes (Cassou et al., 2007). The ubiquity of reemergence in western subtropical and subpolar gyres throughout the World Ocean is now established (Hanawa and

Sugimoto 2004), and strong re-emergence has most recently been highlighted in the southwest Pacific around New Zealand (Ciasto and Thompson, 2009). In an extension of the concept, Sugimoto and Hanawa (2005, 2007) have identified 'remote reemergence' in the North Pacific, whereby sub-surface anomalies re-surface at a more or less remote location in subsequent winters, depending on the strength of advection – in their case study, the swift Kuro Shio current.
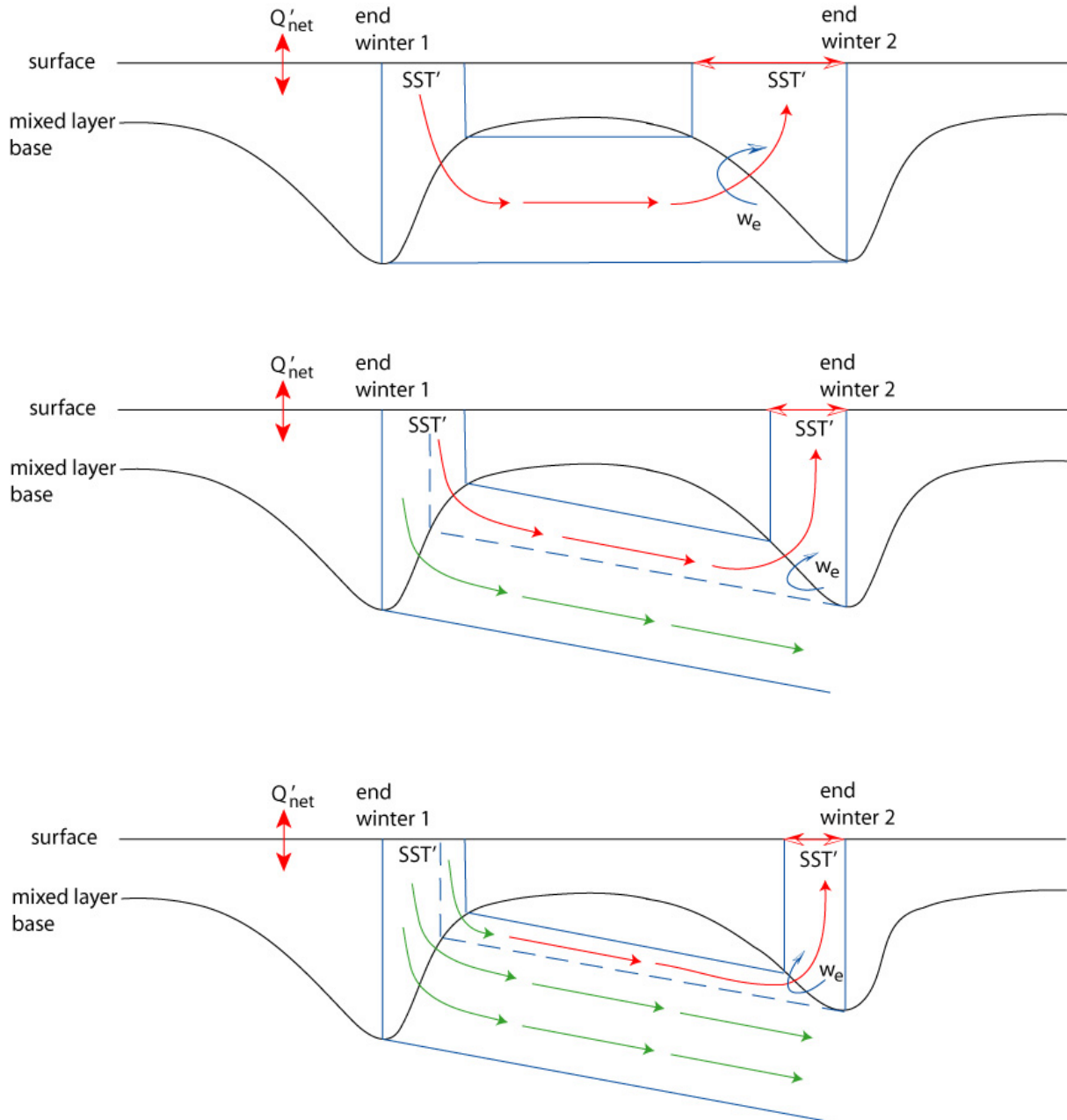

Figure 14. Schematic representations of SST reemergence: (top panel) 'full' reemergence (as in Alexander & Deser 1995); (middle panel) limited reemergence, accounting for downward motion (e.g., Ekman pumping in subtropical gyre); (bottom panel) further limited reemergence, accounting for subduction (horizontal advection or interannual variability in winter mixed layer depth).

The reemergence of SST anomalies is schematically summarized in Fig. 14. The key ingredient is a substantial seasonal cycle in mixed layer depth, typically varying in the range 50-300 m in western subtropical gyres. SST anomalies in winter 1 are mixed well below the surface. Re-stratification and mixed layer shoaling in spring isolates these anomalies in the seasonal thermocline. In the following autumn, the preserved sub-surface temperature anomalies are re-entrained back into the mixed layer, essentially re-emerging at the surface 6-9 months after formation and persisting into winter 2. The top panel in Fig. 14 illustrates the unrealistic instance of 'full' reemergence (as in Alexander and Deser, 1995) as late winter SST anomalies are perfectly preserved. The middle panel illustrates limited reemergence, accounting for downward motion such as Ekman pumping in the subtropical gyre. As a result, only SST anomalies formed late in winter 1 re-emerge in winter 2, with anomalies from earlier in winter 1 subducting beneath the mixed layer in winter 2. The bottom panel illustrates even more limited reemergence, in this case due to a shallower mixed layer depth in winter 2. This may arise through horizontal advection to a location where the seasonal cycle is less extreme, or through interannual variability of winter mixed layer depth (in the absence of advection). As mentioned in Section 2, subduction zones are ubiquitous throughout the subtropical gyres (see Fig. 15), restricting the extent of reemergence in these regions.
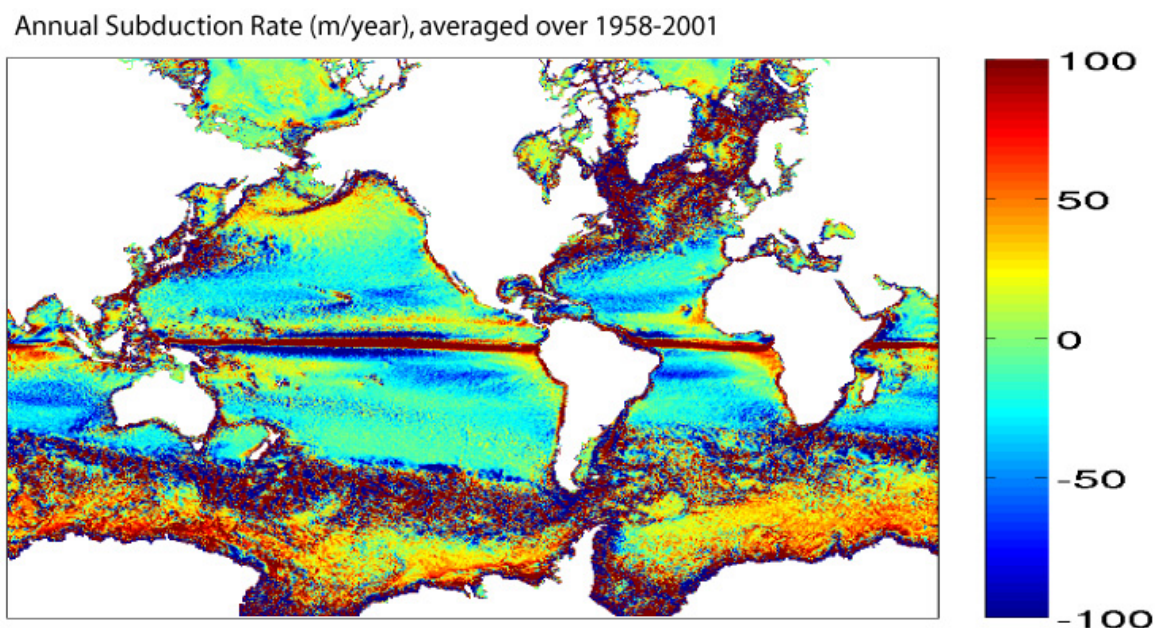

Figure 15. Subduction/Obduction ((m/year, negative/positive respectively) to/from the thermocline in 1/4° NEMO hindcast for 1958-2001 (Figure courtesy Sarah Taws, NOCS).

Complementary to the observational studies cited above, ocean models have been used in a variety of ways to explore reemergence (Junge and Haine, 2001; De Coëtlogon and Frankignoul, 2003; Zhao and Haine, 2005). In particular, models provide an ideal framework for establishing how strong advection accounts for the extended persistence of SST anomalies, e.g., along the path of the Gulf Stream, where winter SST anomalies may persist up to 3 years after surface formation (de Coëtlogon and Frankignoul 2003). In the context of seasonal predictability, Rodwell and Folland (2002) established a statistical basis for using May SST anomalies in the seasonal forecast system of the UK Met Office. A clearer understanding of the associated reemergence process in NEMO – the ocean component of the dynamical forecast system at the Met Office – is therefore desirable. While much innovative diagnosis has been undertaken to explore the reemergence mechanism in different models, there is scope to exploit novel Lagrangian methods such as the offline trajectory analysis previously used to diagnose transport on long timescales (see Section 2).

In reality, mixing due to mesoscale eddies will strongly disperse temperature anomalies prior to reemergence, while atmospheric forcing will further reduce the influence of re-emerging temperature anomalies on SST variability. Diagnosis of the reemergence process has so far been restricted to ocean models of low horizontal resolution. Preliminary analysis of reemergence in NEMO at both 1° and 1/4° (eddy-permitting) resolution reveals that eddies indeed disrupt the process. The potential impact of higher ocean resolution on seasonal forecast skill is presently unclear.

6.   Systematic SST Errors in Ocean Models

The simulation of SST variability in ocean models is to a large extent contingent on the realism of the model climatology. An enduring problem in ocean models is the representation of the unresolved processes that strongly influence water mass properties, the 3-dimensional density field, and the associated large-scale circulation. The consequent misplacement of major ocean currents ultimately leads to large systematic SST errors. Two unresolved processes, turbulent mixing and deep overflows, are often inextricably linked, an example being the boundary current system of the North Atlantic subpolar gyre (Lauderdale et al. 2008). In a model-data comparison exercise, transports across a section through the subpolar gyre are partitioned according to potential temperature and salinity. Observed transports across the section are compared to those diagnosed in the 1/4° version of OCCAM (Fig. 16). The differences are subtle, but the model southward flow is too warm and salty, indicating misrepresentation of the aforementioned processes.

Further south, the North Atlantic Current in OCCAM is too zonal in the vicinity of the Grand Banks off Newfoundland – an oceanographic region known as the 'Northwest Corner'. As a consequence, cold and fresh subpolar water extends into a region where warm and salty water prevails in the real world, revealed as negative long-term differences between model and observed SST (Fig. 17). SST errors are reduced to an extent by increasing model resolution, in OCCAM from 1/4° to 1/12° (see Fig. 17a,b). The higher resolution simulation features more realistic boundary currents, fronts and eddy fluxes, but substantial SST errors persist in the Northwest Corner. OCCAM is typical of z-coordinate models in this regard. While next generation climate models admit eddy-permitting ocean resolution, SST errors such as those in the Northwest Corner likewise persist (e.g., Shaffrey et al. 2009).
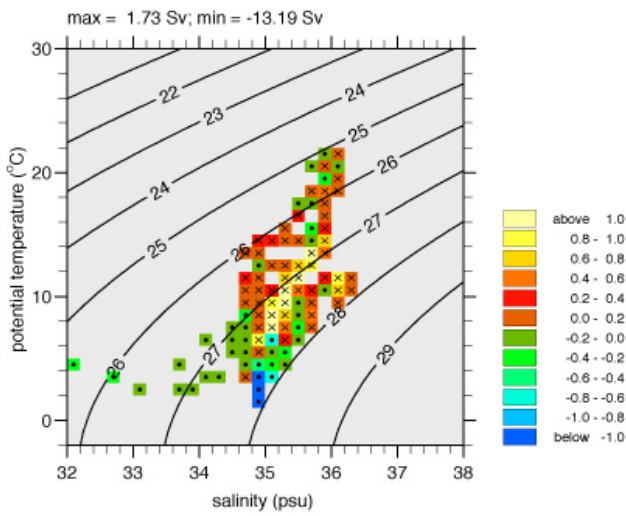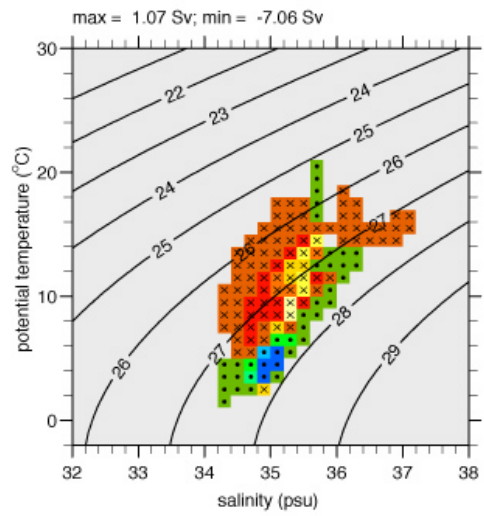
Figure 16. Northward transport (Sv) across a section from Spain to Greenland, partitioned in potential temperature and salinity: (a) observations; (b) 1/4° OCCAM hindcast for 1985-2002 (Marsh et al. 2005).

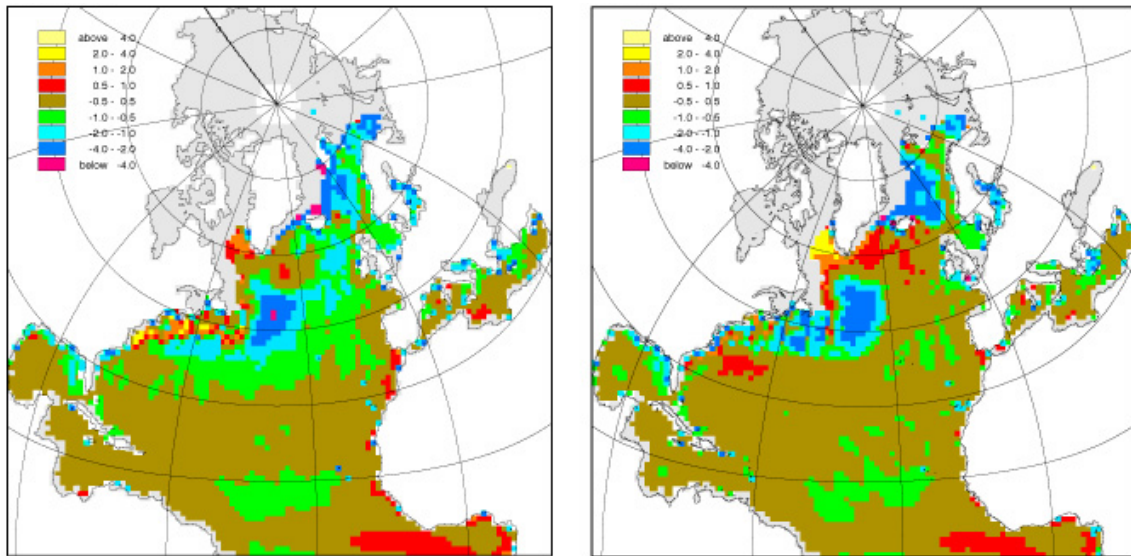*Figure 17. SST errors in 1/4° and 1/12° versions of OCCAM (left and right panels respectively), defined as model minus NOCS observations (ship-based measurements) using monthly-mean SST for 1985-2003 (Marsh et al. 2009).*

7. Summary and Conclusions

The focus of this contribution has been on the active role of the ocean in the variability of SST in the extratropics, highlighting some of the processes by which this variability may arise. A range of ocean GCMs and diagnostics is available to represent and investigate these processes. During the last decade, OGCMs have reached unprecedented high resolution, finally resolving mesoscale eddies at the global scale. Through the combination of higher resolution, improved physical and numerical schemes, and more accurate surface boundary conditions, OGCM simulations have become steadily more realistic. Such simulations yield datasets that grow larger with resolution, challenging standard diagnostic approaches. During the same decade, observations and sampling of the 3-dimensional ocean have likewise developed. Fresh interpretations of archived hydrographic data provide a clearer picture of slow changes over last 50 years, such as a multi-decadal cycle in the Atlantic. Satellite measurements of sea surface height since 1992 provide a lengthening time series of the spatial pattern of changing upper ocean heat content, while Argo measurements since 1999 are now being used in analyses of interannual variability in ocean inventories and transports. Finally, MOC monitoring since April 2004 is yielding a unique new time series of this key component of the large-scale ocean circulation.

Two processes and respective timescales have been highlighted: interannual to decadal variability of the MOC and associated heat transport; seasonal to interannual reemergence of SST anomalies formed in previous winters, modified by subduction, advection and eddies. SST anomalies may be further associated with coupled modes of variability involving changes in gyre and Ekman transport. There is some evidence for links between different processes and timescales. For example, SST anomaly reemergence in the North Pacific is observed to strengthen and diminish with the Aleutian Low on a decadal timescale (Sugimoto and Hanawa, 2007). While much of this SST variability is potentially predictable, the anticipated skill of seasonal to decadal climate forecasts is contingent on the realism of these processes in dynamical models. A wide range of ocean model diagnostics has been used to address this issue, but there is scope for further innovation. In particular, Lagrangian diagnostics may more clearly establish the link between SST variability and earlier remote SST anomalies. One remaining caveat concerns the systematic SST errors that persist at even eddy resolution in key regions such as the 'Northwest Corner', and the implications for SST variability. Reliable climate forecasting may yet depend on fundamental advances in ocean modeling that lead to the elimination of these errors.

Acknowledgements

References

Alexander, M. A., and C. Deser (1995). A mechanism for the recurrence of wintertime midlatitude SST anomalies. *J. Phys. Oceanogr.*, **25**, 122-137.

Alexander, M. A., Deser, C., and M. S. Timlin (1999). The reemergence of SST anomalies in the North Pacific Ocean. *J. Climate*, **12**, 2419-2433.

Alexander, M. A., Timlin, M. S., and J. D. Scott (2001). Winter-to-winter recurrence of sea surface temperature, salinity and mixed layer depth anomalies. *Progress in Oceanography*, Vol. **49**, Pergamon, 41-61.

Balmaseda, M. A., Smith, G. C. Haines, K., Anderson, D., Palmer, T. N., and A. Vitard (2007). Historical reconstruction of the Atlantic meridional overturning circulation from the ECMWF operational ocean reanalysis. *Geophys. Res. Lett.*, **34**, L23615, doi: 10.1029/2007GL031745.

Bleck, R. (2002). An oceanic general circulation model framed in hybrid isopycnic-cartesian coordinates. *Ocean. Modelling*, **4**, 55–88.

Bryden, H. L., and S. Imawaki. (2001). Ocean heat transport, in *Ocean Circulation and Climate*, edited by G. Siedler, J. Church and J. Gould, Academic Press, 455-474.

Bryden, H. L., Longworth, H. R., and S. A. Cunningham (2005). Slowing of the Atlantic meridional overturning circulation at 25ºN. *Nature*, **438**, 655-657.

Cassou, C., Deser, C., and M. A. Alexander (2007). Investigating the impact of reemerging sea surface temperature anomalies on the winter atmospheric circulation over the North Atlantic. *J. Climate*, **20**, 3510-3526.

Ciasto, L. M., and D. W. J. Thompson (2009). Observational evidence of reemergence in the extratropical Southern Hemisphere. *J. Climate*, **22**, 1446-1453.

De Coëtlogon, G., and C. Frankignoul (2003). The persistence of winter sea surface temperature in the North Atlantic. *J. Climate*, **16**, 1364-1377.

Deser, C., Alexander, M. A., and M. S. Timlin (2003). Understanding the persistence of sea surface temperature anomalies in mid-latitudes. *J. Climate*, **16**, 57-72.

Deser, C., Alexander, M. A., Xie, S.-P., and A. S. Phillips. Sea Surface Temperature Variability: Patterns and Mechanisms, *Annual Review of Marine Sciences*, submitted.

Frankignoul, C., and K. Hasselmann (1977). Stochastic climate models. Part 2. Application to sea surface temperature variability and thermocline variability. *Tellus*, **29**, 289-305.

Grist, J. P., Marsh, R., and S. A. Josey (2009). On the Relationship Between the North Atlantic Meridional Overturning Circulation and the Surface-Forced Overturning Stream Function. *Journal of Climate*, in press.

Grist, J. P., et al. (2010). The roles of surface heat flux and ocean heat transport during four decades of Atlantic Ocean temperature variability. *Ocean Dynamics* (10.1007/s10236-010-0292-4)

Hanawa, K., and S. Sugimoto (2004). 'Reemergence' areas of winter sea surface temperature anomalies in the world's oceans. *Geophys. Res. Lett.*, **31**, L01303, doi:10.1029/2004GL019904.

Ivchenko V. O., Wells, N. C., and D. L. Aleynik (2006). Anomaly of heat content in the Northern Atlantic in the last 7 years: is the ocean warming or cooling? *Geophysical Research Letters*, **33**, L22606.

Ivchenko, V. O., et al. (2007). Comparing of the steric height in the Northern Atlantic with the satellite altimetry. *Ocean Science*, **3**, 485-490.

Josey, S. A., Grist, J. P., and R. Marsh (2009). Estimates of Meridional Overturning Circulation Variability in the North Atlantic from Surface Density Flux Fields. *Journal of Geophysical Research,* in press.

Junge, M. M., and T. W. N. Haine (2001). Mechanisms of North Atlantic wintertime sea surface temperature anomalies. *J. Climate*, **14**, 4560-4572.

Lauderdale, J. M., Bacon, S., Naveira Garabato, A. C. and Holliday, N. P. (2008). Intensified turbulent mixing in the boundary current system of southern Greenland. *Geophys. Res. Lett.*, **35**, L04611. (doi:10.1029/2007GL032785).

Lumpkin, R., and K. Speer (2007). Global ocean meridional overturning. *J. Phys. Oceanogr.*, **37**, 2550-2562.

Marsh, R. (2000). Recent variability of the North Atlantic thermohaline circulation inferred from surface heat and freshwater fluxes. *J. Climate*, **13**, 3239-3260.

Marsh, R., Nurser, A.J.G., Megann, A.P. and A. L. New (2000). Water mass transformation in the Southern Ocean of a global isopycnal coordinate GCM. *J. Phys. Oceanogr.*, **30**, 1013-1045.

Marsh, R. and A. P. Megann (2002). Tracing water masses with particle trajectories in an isopycnic-coordinate model of the global ocean. *Ocean Modelling*, **4**, (1), 27-53. (doi:10.1016/S1463-5003(01)00011-7).

Marsh, R., Josey, S.A., Nurser, A.J.G., de Cuevas, B.A. and A. C. Coward (2005). Water mass transformation in the North Atlantic over 1985-2002 simulated in an eddy-permitting model. *Ocean Science*, **1**, (2), 127-144. (SRef-ID: 1812-0792/os/2005-1-127).

Marsh, R., Josey, S.A., de Cuevas, B.A., Redbourn, L.J. and Quartly, G.D. (2008) Mechanisms for recent warming of the North Atlantic: Insights gained with an eddy-permitting model. *Journal of Geophysical Research*, **114**, (C4), C04031. (doi:10.1029/2007JC004096)

Marsh, R., de Cuevas, B. A., Coward, A. C., Jacquin, J., Hirschi, J. J.-M., Aksenov, Y., Nurser, A.J. G., and S. A. Josey (2009). Recent changes in the North Atlantic circulation simulated with eddy-permitting and eddy-resolving ocean models. *Ocean Modelling*, **28**, (4), 226-239. (doi:10.1016/j.ocemod.2009.02.007).

Namias, J., and R. M. Born (1970). Temporal coherence in North Pacific sea surface temperature patterns. *J. Geophys. Res.*, **75**, 5952-5955.

Namias, J., and R. M. Born (1974). Further studies of temporal coherence in North Pacific sea surface temperatures. *J. Geophys. Res.*, **79**, 797-798.

New, A. L., Bleck, R., Jia, Y., Marsh, R., Huddleston, M., and S. Barnard (1995). An isopycnic model study of the North Atlantic. Part I: Model experiment. *J. Phys. Oceanogr.*, **25**, 2667-2699.

Pain C. C., Piggott M. D., Goddard A. J. H., Fang F., Gorman G. J., Power P. W., and C. R. E. de Oliveira (2005). Three-dimensional unstructured mesh ocean modelling. *Ocean Modelling*, **10**, 5–33. doi:10.1016/j.ocemod.2004.07.005.

Piggott M. D., Gorman G. J., Pain C. C., Allison P. A., Candy A. S., Martin B. T., and M. R. Wells (2008). A new computational framework for multi-scale ocean modelling based on adapting unstructured meshes. *Int. J. Numer. Methods Fluids*, **56**, 1003–1015. doi:10.1002/fld.1663.

Rodwell, M. J., and C. K. Folland (2002). Atlantic air-sea interaction and seasonal predictability. *Quart. J. Roy. Met. Soc.*, **128**, 1413-1443.

Shaffrey, L. C., and 24 others (2009). U.K. HiGEM: The new U.K. high-resolution global environment model – Model description and basic evaluation. *J. Climate*, **22**, 1861-1896.

Sugimoto, S., and K. Hanawa (2005). Remote reemergence areas of winter sea surface temperature anomalies in the North Pacific. *Geophys. Res. Lett.*, **32**, L01606, doi:10.1029/2004GL021410.

Sugimoto, S., and K. Hanawa (2007). Impact of remote reemergence of the subtropical mode water on winter SST variation in the central North Pacific. *J. Climate*, **20**, 173-186.

Timlin, M. S., Alexander, M. A., and C. Deser (2002). On the reemergence of North Atlantic SST anomalies. *J. Climate*, **15**, 2707-2712.

Williams, R. G., Spall, M. A., and J. C. Marshall (1995). Does Stommel's mixed layer 'demon' work? *J. Phys. Oceanogr.*, **25**, 3089-3102.

Zhao, B., and T. W. N. Haine (2005). On processes controlling seasonal North Atlantic sea surface temperature anomalies in ocean models. *Ocean Modelling*, **9**, 211-229.